Comparative Study of the Gel Phases of Ether- and Ester-Linked Phosphatidylcholines†

M. J. Ruocco, D. J. Siminovitch, and R. G. Griffin*

Francis Bitter National Magnet Laboratory, Massachusetts Institute of Technology, Cambridge, Massachusetts 02139

Received August 21, 1984

ABSTRACT: Calorimetric, X-ray diffraction, and ^{31}P nuclear magnetic resonance (NMR) studies of aqueous dispersions of 1,2-dihexadecyl-*sn*-glycero-3-phosphocholine (DHPC) gel phases at low temperatures (−60 to 22 °C) show thermal, structural, and dynamic differences when compared to aqueous dispersions of 1,2-dipalmitoyl-*sn*-glycero-3-phosphocholine (DPPC) gel phases at corresponding temperatures. Differential scanning calorimetry of DHPC dispersions demonstrates a *reversible*, low-enthalpy "subtransition" at 4 °C in contrast to the *conditionally reversible*, high-enthalpy subtransition observed at 17 °C for annealed DPPC bilayers. X-ray diffraction studies indicate that DHPC dispersions form a lamellar gel phase with $d_{av} \simeq$ 46 Å both above and below the "subtransition". It is suggested that the reduced d_{av} observed for DHPC (46 Å as compared to 64 Å in DPPC) is due to an interdigitated lamellar gel phase which exists at all temperatures below the pretransition at 35 °C. ^{31}P NMR spectra of DHPC gel-phase bilayers show an axially symmetric chemical shift anisotropy powder pattern which remains sharp down to −20 °C, suggesting the presence of fast axial diffusion. In contrast, ^{31}P spectra of DPPC bilayers indicate this type of motion is frozen out at ~0 °C.

Following the initial studies of the 1960's in which a link between elevated membrane ether phospholipids and tumor growth was suggested, there has been an increasing interest in the structure and function of these lipids in mammalian membranes. Additional justification for this interest has been provided by recent studies which show a correlation between increased levels of ether-linked phospholipids and neoplasia (Howard et al., 1972, 1973; Albert & Anderson, 1977). Although ether lipids generally occur in minor amounts in such tissues as the intestinal mucosa, significant concentrations of plasmalogens (alkenylacylglycerophospholipids) are found in the brain and myelin membrane (Rouser & Yamamoto, 1968; Norton, 1981). The effects of ether-linked phospholipid structure on cell membranes are presently ill-defined and virtually unknown. This dearth of information has provided the impetus for a number of recent studies which have attempted to characterize the thermal behavior (Vaughan & Keough, 1974; Sunder et al., 1978; Lee & Fitzgerald, 1980), membrane permeability (Schwarz & Paltauf, 1977; Bittman et al., 1981), conformation (Hauser et al., 1981; Hauser, 1981), and molecular packing (Paltauf et al., 1971; Boggs et al., 1981; Lakowicz & Hogen, 1981) of ether phospholipids. Schwarz et al. (1976) demonstrated that hydrated bilayer membranes of homogeneously acylated and alkylated phosphatidylcholine (PC)[1] had different partial specific volumes but exhibited no significant structural differences in bilayer membranes. ^{31}P NMR line shapes of hydrated dihexadecyl-*sn*-glycero-3-phosphocholine (DHPC) bilayer membranes in the gel phase (T = 31 °C) and melted liquid-crystalline phase (T = 50 °C) indicated that the dynamic properties and conformation of the phosphate moiety are insensitive to the glycerol backbone linkages (Hauser, 1981). The author has also shown, using an analysis of ^{1}H spin–spin coupling constants, that the replacement of the ester linkages by ether bonds has no significant effect on the average conformation and segmental motion of the polar group of phosphatidylcholine as monomers in solution or in micelles.

In contrast to these studies, which demonstrated conformational and motional similarities of ester and ether phosphatidylcholine aggregates in the L_α phases, wide-line ^{14}N NMR experiments have provided evidence for significant dynamic differences between DPPC and DHPC in the low-temperature gel phases (Siminovitch et al., 1983). Specifically, in DPPC the ^{14}N spectrum broadens beyond detectability at ~0 °C, whereas for DHPC this same phenomenon does not occur until −20 °C. The possibility also exists for the formation of stable, low-temperature lamellar "crystal" phases in DHPC, as occurs in DPPC bilayers (Füldner, 1981; Ruocco & Shipley, 1982a,b). Because of the ^{14}N NMR observations, and the fact that low-temperature gel bilayer dispersions would more readily manifest thermal, structural, and conformational differences between ester- and ether-linked lipids, we undertook a study to characterize DHPC lamellar gel phases which could then be compared to the DPPC lamellar gel phases.

Materials and Methods

Synthetic DHPC and DPPC (Calbiochem-Behring Corp., La Jolla, CA) were purified by silicic acid chromatography and shown to be >99% pure by thin-layer chromatography. Lipid dispersions containing 50 wt % water were prepared for DSC, X-ray diffraction, and ^{31}P NMR. Lipid dispersions were equilibrated at $T > T_c$ (phospholipid), cooled to room tem-

† This research was supported by the National Institutes of Health (Grants GM-25505, GM-23289, and RR-00995) and by the National Science Foundation through its support of the Francis Bitter National Magnet Laboratory (Grant DMR-8211416). D.J.S. and M.J.R. are recipients of postdoctoral fellowships from the Natural Sciences and Engineering Research Council of Canada and the National Multiple Sclerosis Society (FG591-A-1), respectively. A preliminary account of this work was presented at the 28th Annual Biophysical Society Meeting in San Antonio, TX (Siminovitch et al., 1984).

[1] Abbreviations: PC, phosphatidylcholine; NMR, nuclear magnetic resonance; DHPC, 1,2-dihexadecyl-*sn*-glycero-3-phosphocholine; DPPC, 1,2-dipalmitoyl-*sn*-glycero-3-phosphocholine; DSC, differential scanning calorimetry.

0006-2960/85/0424-2406$01.50/0

Table I: Transition Temperatures and Enthalpies of Hydrated DPPC and DHPC

	first heating scan		cooling scan		reheating scan	
	T_c (°C)	ΔH (kcal/mol)	T_c (°C)	ΔH (kcal/mol)	T_c (°C)	ΔH (kcal/mol)
			(A) DPPC/H_2O (50 wt % H_2O)			
subtransition	16.7	3.7				
pretransition	33.5	1.2	30.4	0.6	33.5	1.2
main transition	41.2	8.6	41.2	8.9	41.5	8.6
			(B) DHPC/H_2O (50 wt % H_2O)			
"subtransition"	4[a]	0.5	2[a]	0.5	4[a]	0.5
pretransition	34.8	1.6	31.8	1.3	34.8	1.6
main transition	43.7	9.4	43.7	9.7	43.7	9.5

[a] Peak temperature of transition.

perature, and stored at −5 °C for periods ≥2 days prior to experiments. In some instances, no low-temperature equilibration or longer equilibration periods and/or lower temperatures were used to see if significant thermal and structural changes developed. Following storage, lipid dispersions were transferred at low temperatures to the scanning calorimeter, X-ray camera, or NMR probe. Differential scanning calorimetry was performed by using a DSC-2 calorimeter (Perkin-Elmer, Norwalk, CT) over the −10 to 53 °C range at 5 °C/min. X-ray diffraction measurements were performed by using Cu Kα X-radiation from a microfocus X-ray generator (Jarrell-Ash, Waltham, MA) which was line focused by a single mirror and collimated by using the slit optical system of a Luzzati-Baro camera (E^{TS}, Beaudouin, Paris, France). X-ray diffraction patterns were recorded with a linear position sensitive detector (Tennelec, Oak Ridge, TN) and associated electronics (Tracor Northern, Middleton, WI). Lipid dispersions were sealed in capillary tubes (i.d. = 1 mm) (Charles Supper Co., Natick, MA).

^{31}P NMR spectra were obtained on home-built solid-state pulse spectrometers operating at either 6.8 or 7.3 T, corresponding to ^{31}P frequencies of 119 or 128 MHz, respectively. NMR experiments were performed by using a high-power probe with an 8-mm solenoidal sample coil which was doubly tuned for ^{31}P and ^{1}H. To avoid distortions in the line shape which would result from the use of normal single pulse techniques, all NMR spectra were obtained by using a Hahn echo (Wittebort et al., 1981; Rance & Byrd, 1983). Typical 90° pulses were 8 μs in duration and were separated by a pulse spacing (τ) of 60 μs. The recycle time varied between 2 and 5 s, which in all cases was long enough to prevent any significant heating from the ^{1}H decoupling field. The Hahn echo signal was digitized at 5 μs/point, corresponding to a spectral width of ±100 kHz. To enhance the signal to noise ratio, typically 4–8K scans were signal averaged.

Results

DSC. Representative calorimetric thermograms of annealed DHPC/water and DPPC/water (50 wt %) dispersions are shown in Figure 1. Following 2-days incubation at −5 °C, the initial heating scan at 5 °C/min of DPPC/water bilayer dispersions reveals three transitions at 16.7 °C (subtransition), 33.5 °C (pretransition), and 41.2 °C (main transition) (Figure 1A). The subtransition corresponds to the $L_c \rightarrow L_{\beta'}$ gel bilayer transformation (Ruocco & Shipley, 1982a,b) and exhibits an enthalpy of 3.7 kcal/mol of DPPC. The $L_{\beta'} \rightarrow P_{\beta'}$ and $P_{\beta'} \rightarrow L_\alpha$ bilayer transitions yield enthalpies of 1.2 and 8.6 kcal/mol of DPPC, respectively. Immediate cooling from 53 to −8 °C demonstrates that the main transition (T_c = 41.2 °C; ΔH = 8.9 kcal/mol of DPPC) and pretransition (T_c = 30.4 °C; ΔH = 0.6 kcal/mol of DPPC) are reversible (Figure 1B). The observed thermal hysteresis of the $P_{\beta'} \rightarrow L_{\beta'}$ conversion in Figure 1B has been recently characterized in a kinetic study

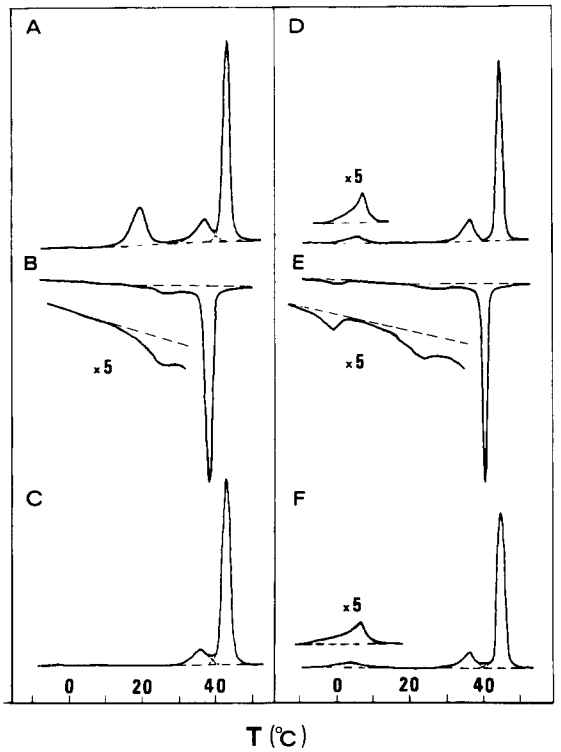

FIGURE 1: DSC thermograms of DPPC/water (A–C) and DHPC/water (D–F) (50 wt %) dispersions following equilibration at −5 °C for 2 days. DPPC: (A) Initial heating run following storage at −5 °C; (B) cooling run performed immediately after (A); (C) heating run performed immediately after (B). DHPC: (D) Initial heating run following storage at −5 °C; (E) cooling run performed immediately after (D); (F) heating run performed immediately after (E). Programming rate for all scans = 5 °C/min.

by Cho et al. (1981). In contrast, the subtransition is not reversible. The recrystallization of the low-temperature L_c bilayer phase and the L_c "crystal" $\rightarrow L_{\beta'}$ gel bilayer thermal parameters obtained are subject to thermal and equilibration requirements as described earlier (Chen et al., 1980; Füldner, 1981; Ruocco & Shipley, 1982a,b; Serrallach et al., 1983). Immediate reheating from −8 °C yields no apparent low-temperature gel → gel transformation, while the pretransition and main transition are again observed (Figure 1C) (also see Table IA for thermal parameters).

The thermal behavior of DHPC/water dispersions following identical annealing conditions also exhibits three transitions at 4 °C (low-temperature lamellar gel → gel transformation, hereafter referred to as the "subtransition"), 34.8 °C (pretransition), and 43.7 °C (main transition) (Figure 1D). Enthalpy measurements show that the "subtransition" is of low enthalpy (ΔH = 0.5 kcal/mol of DHPC). Enthalpy data for the high-temperature transitions are summarized in Table IB and compared to the corresponding thermal data for DPPC

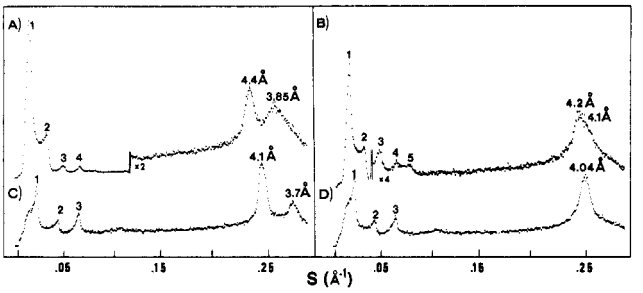

FIGURE 2: X-ray diffraction patterns of DPPC/water and DHPC/water (50 wt %) dispersions following equilibration at −5 °C. (A) DPPC/water dispersions at −2 °C; (B) DPPC/water dispersions at 20 °C; (C) DHPC/water dispersions at −2 °C; (D) DHPC/water dispersions at 20 °C.

bilayers in Table IA. Of some interest is the fact that the subsequent cooling scan (Figure 1E) reveals *all* transitions are reversible, including the "subtransition". Furthermore, the DHPC low-temperature transition is not kinetically limited under the conditions used (see Materials and Methods and below). This is to be contrasted with the cooling behavior of DPPC bilayers (compare scans B and E of Figure 1). Reheating the DHPC dispersion yields results similar to those obtained from the initial heating scan (see Figure 1F and Table IB). Longer annealing periods (>3 days to weeks) at temperatures of −3 to −5 °C resulted in no increase in the "subtransition" enthalpy for DHPC bilayers, whereas after similar annealing conditions in DPPC bilayers, an increase in the subtransition enthalpy was observed, as reported earlier (Magni & Sheridan, 1982; Ruocco & Shipley, 1982b).

X-ray Diffraction. DPPC/water and DHPC/water dispersions were annealed at −5 °C for ≥2 days prior to exposure to X-rays at low temperatures. DPPC gel bilayer X-ray diffraction patterns are shown in scans A and B of Figure 2 at −2 and 20 °C, respectively. The diffraction pattern of the L_c bilayer phase at −2 °C (Figure 2A) contains four lamellar reflections (d_{av} = 59 Å) in the low-angle region (see numbered reflections in Figure 2A). The wide-angle region yields two strong reflections at 1/4.4 and 1/3.85 Å^{-1}. Upon traversing the $L_c \rightarrow L_{\beta'}$ subtransition, the characteristic $L_{\beta'}$ X-ray diffraction pattern exhibiting five lamellar low-angle reflections (d_{av} = 64 Å) and an asymmetric envelope in the wide-angle region consisting of two reflections at 1/4.2 and 1/4.1 Å^{-1} is observed (Figure 2B). These structural observations for DPPC gel bilayers have been well-documented (Tardieu et al., 1973; Janiak et al., 1976; Ruocco & Shipley, 1982a,b). The low-temperature X-ray diffraction pattern at −2 °C taken below the DHPC "subtransition" is shown in Figure 2C. In contrast to the X-ray diffraction pattern observed for DPPC, the DHPC X-ray diffraction pattern exhibits only three low-angle reflections indexing on a much reduced lamellar periodicity of d_{av} = 46.3 Å. Note that the number of lamellar reflections and their intensity distribution differ markedly between the low-temperature DPPC and DHPC gel phases (compare patterns A and C of Figure 1). The reduced lamellar periodicity of the DHPC dispersions is of particular significance: d_{L_c}(ether) = 46.3 Å << d_{L_c}(ester) = 59 Å. In addition to the differences in the low-angle region, the two wide-angle reflections observed for the DHPC gel phase occur at 1/4.1 and 1/3.7 Å^{-1} (compare the wide-angle region of Figure 2C with Figure 2A). It should be noted that heating through the "subtransition" to 20 °C does not result in any significant alteration of the lamellar periodicity (d_{av} = 46.8 Å). Similarly, no significant change in intensity distribution is observed (compare scans C and D of Figure 2). At 20 °C, a single

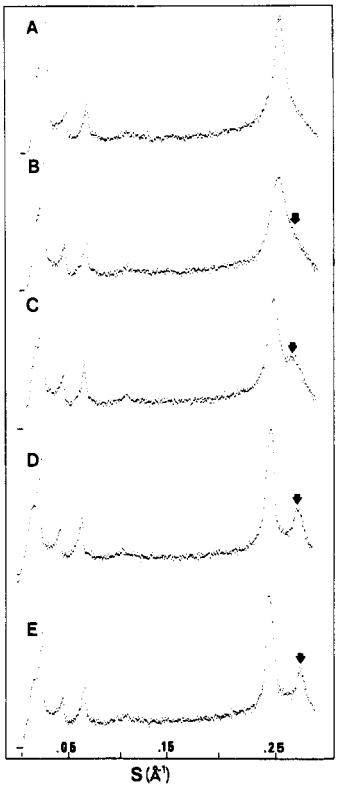

FIGURE 3: X-ray diffraction patterns of a DHPC/water (50 wt %) dispersion as a function of temperature: (A) 20 °C; (B) 10 °C; (C) 5 °C; (D) 0 °C; (E) −2 °C.

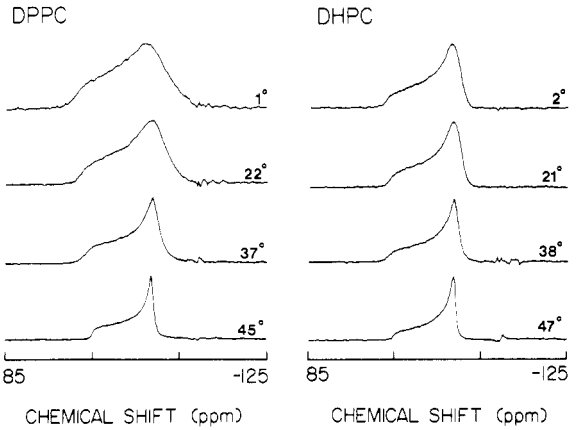

FIGURE 4: Proton-decoupled ^{31}P spectra of hydrated lipids as a function of temperature. Dispersions were *not* incubated at low temperature prior to NMR experiments. Chemical shift is referred to 85% H_3PO_4 as an external standard.

wide-angle reflection at 1/4.04 Å^{-1} is recorded. The temperature-dependent X-ray diffraction patterns in Figure 3 show that with increasing temperature the two wide-angle reflections at 1/4.1 and 1/3.7 Å^{-1} move toward smaller and larger spacings, respectively, until a symmetric reflection is obtained at 20 °C. In agreement with the thermal behavior of the DHPC dispersions, these structural changes detected by X-ray diffraction are completely reversible upon cooling and reheating.

^{31}P NMR. Figures 4 and 5 display the proton-decoupled ^{31}P NMR spectra of DPPC and DHPC at representative temperatures in the three gel and liquid-crystalline phases. The DPPC spectra of Figure 4 were obtained from samples which were *not* incubated for prolonged periods at low temperatures prior to the NMR experiments. The DPPC spectrum obtained at 1 °C is very similar to that previously reported by Füldner

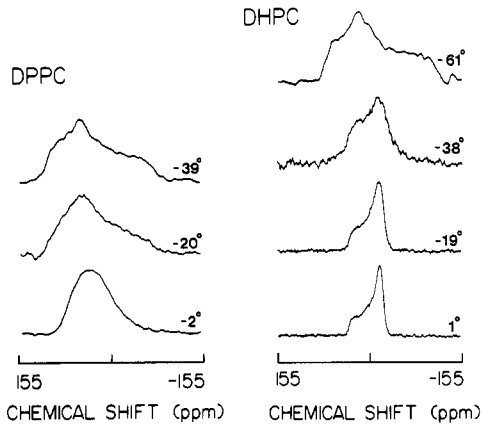

FIGURE 5: Proton-decoupled ^{31}P spectra of hydrated lipids as a function of temperature. Dispersions were incubated at low temperature (−5 °C) prior to NMR experiments.

Table II

DPPC		DHPC	
T (°C)	$\Delta\sigma$ (ppm)	T (°C)	$\Delta\sigma$ (ppm)
45	48	47	48
37	57	38	53
22	63	21	55
1	65	2	56
		−19	56

(1981) from unannealed DPPC liposomes at 5 °C and reflects the fact that the $L_{\beta'}$ phase has not yet converted into the more ordered bilayer structure characteristic of the subphase (Ruocco & Shipley, 1982a). The amorphous line shape of DPPC at −2 °C in Figure 5 demonstrates that prolonged incubation at a temperature of −5 °C will allow the dispersion to anneal into the stable crystal bilayer form of the subphase. Such a line shape has previously been observed by Füldner (1981) from annealed DPPC liposomes at 5 °C, and by Lewis et al. (1984) from annealed liposomes at 2 °C.

The spectra from both lipids in the L_α phase are axially symmetric powder pattern line shapes. As previously reported (Hauser, 1981; Siminovitch et al., 1983), neither the line shapes nor the magnitudes of the chemical shift anisotropies (see Table II) are significantly different in the liquid-crystalline phase. In the spectra of the $P_{\beta'}$ phase of both lipids, there is a simultaneous increase in spectral broadening and in the chemical shift anisotropy. As in the L_α phases, the line shapes of the $P_{\beta'}$ phase at 37–38 °C are very similar, consistent with the observation by Hauser (1981) that the ^{31}P line shapes of DPPC and DHPC at 31 °C are superimposable. Both the magnitude of the chemical shift anisotropy and the spectral broadening increase significantly in the $L_{\beta'}$ phase of DPPC. However, Figure 5 shows that at lower temperatures in the gel phase, DPPC and DHPC give rise to distinctly different NMR line shapes. At −20 °C in annealed DPPC liposomes, the ^{31}P powder pattern has clearly undergone a reversal in the sign of the chemical shielding anisotropy and approaches the axially asymmetric rigid lattice line shape observed at −39 °C. In contrast, axially *symmetric* powder patterns are observed in the gel phase of DHPC until −20 °C; remarkably, the magnitude of the chemical shift anisotropy (Table II) changes by less than 3 ppm over the 57 °C range from 38 (53 ppm) to −19 °C (56 ppm). By −38 °C, the axially symmetric line shape has undergone significant broadening due to reduced motional averaging, but the sign of the chemical shielding anisotropy remains unchanged. It is not until −61 °C that the axially asymmetric line shape characteristic of a rigid-lattice ^{31}P chemical shielding tensor is observed.

Discussion

DSC of DHPC/water dispersions clearly indicates the presence of a *reversible*, low-temperature transition (T_{peak} = 4 °C) (Figure 1). This is in contrast to the *conditionally reversible* subtransition of DPPC bilayers. As reported previously by Vaughan & Keough (1974), the "pretransition" and main hydrocarbon chain order–disorder transition occur at slightly higher temperatures than the DPPC pretransition and main transition (compare parts A and B of Table I). Because the DHPC and DPPC dispersions demonstrated very different thermal behavior at low temperatures (≤25 °C), our initial structural and dynamic studies have concentrated on the gel subphases.

X-ray diffraction data above and below the "subtransition" in DHPC demonstrate that there are no significant changes in the lamellar periodicity or in the distribution of reflection intensities at low angles [see S (Å^{-1}) < 0.15 in Figure 2C,D]. At −2 °C, the wide-angle reflections in Figure 2C are characteristic of a simple orthorhombic hydrocarbon chain packing mode (Lutton, 1950; Hoerr & Paulicka, 1968). Heating from −2 °C through the "subtransition" to 20 °C results in a hydrocarbon chain packing rearrangement which yields a single, sharp symmetric reflection at 1/4.04 Å^{-1}. This X-ray diffraction pattern is characteristic of lamellae having hydrocarbon chains of the lipid in a hexagonally packed two-dimensional lattice, with no molecular tilt (Tardieu et al., 1973). The insignificant intensity and positional changes of the low-angle reflections vs. the positional and intensity changes of the wide-angle reflections (see Figure 3) suggest that the DHPC "subtransition" involves a two-dimensional in-plane polymorphic hydrocarbon chain packing transition from an orthorhombic subcell to a hexagonal subcell. Similar ^{31}P NMR spectral line shapes above (+2 °C) (Figure 4) and below (−19 °C) (Figure 5) the "subtransition" indicate that the phosphocholine head group is relatively insensitive to these packing changes. This behavior suggests that the "subtransition" in DHPC involves primarily a hydrocarbon chain packing rearrangement, without any significant changes in head-group hydration, unlike the DPPC subtransition which involves changes in *both* hydration *and* chain packing (Ruocco & Shipley, 1982b). ^{31}P NMR line shapes above (22 °C) (Figure 4) and below (−2 °C) (Figure 5) the subtransition in DPPC bilayer dispersions clearly indicate differences in the amount of motional averaging of the ^{31}P chemical shielding interaction. These differences are probably attributable to "crystallization" of DPPC and tightly bound water molecules at the subtransition to form an ordered interbilayer matrix characterized by water/water and water/DPPC hydrogen bonding (Ruocco & Shipley, 1982b).

Under appropriate conditions, the DPPC bilayer subtransition enthalpy is as high as ~7 kcal/mol of DPPC (Magni & Sheridan, 1982; Ruocco & Shipley, 1982b; Serrallach et al., 1983). Equilibration conditions used to date (i.e., prolonged storage ≤2 weeks at −26 or −5 °C) have resulted in neither a difference in the thermal behavior of DHPC bilayers reported above nor an enhancement of the DHPC "subtransition" enthalpy. An increase in enthalpy similar to that observed in DPPC bilayers may not be expected for DHPC lamellae if the "subphase" gel → gel transition involves primarily chain packing and not significant hydration changes.

The most interesting structural feature that emerges from this initial study of DHPC is the reduced lamellar periodicity of 46 Å for which there are two possible explanations: (1) an extreme DHPC molecular tilt relative to the bilayer normal,

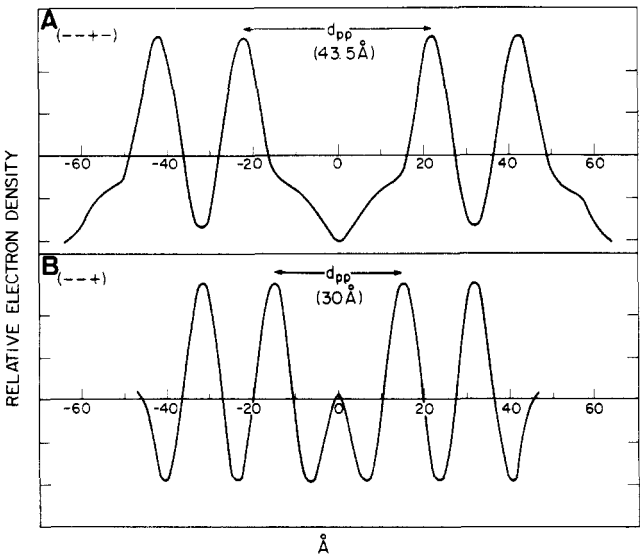

FIGURE 6: Electron density profiles of the DHPC interdigitated lamellar gel phase at 20 °C; d_{pp} is the intrabilayer peak to peak separation; structure factor amplitude phases are indicated in parentheses.

or (2) an interdigitated lamellar phase. Analysis of the X-ray diffraction data favors the latter explanation for the following reasons. First, the very presence of sharp, symmetrical wide-angle reflections indicates that the two-dimensional hydrocarbon lattice involves parallel packing of the alkyl chains, all of which are oriented at right angles to the plane of the bilayer (Tardieu et al., 1973). Scattering of this nature would not be expected for hydrocarbon chains tilted with respect to the bilayer [see Tardieu et al. (1973)]. Second, lamellar periodicities on the order of 38–50 Å and sharp, symmetrical wide-angle reflections have been shown to be characteristic features of interdigitated lamellar phases (Ranck et al., 1977; Serrallach et al., 1983; McIntosh et al., 1983; McDaniel et al., 1983). In particular, McIntosh and colleagues have recently demonstrated the induction of interdigitated DPPC lamellar phases by nonelectrolytes (McDaniel et al., 1983; McIntosh et al., 1983) which have lamellar periodicities between 40 and 50 Å and lipid thickness (d_l) of 30 Å. The d spacings are similar to those observed for DHPC ($d \sim 46$ Å) in the lamellar gel phases above (20 °C) and below (−2 °C) the "subtransition". Third, the structure factor amplitudes calculated from the low-angle lamellar reflection intensities of both DHPC gel phases fit the structure factor amplitude vs. reciprocal space curve in Figure 1 of McIntosh et al. (1983). Figure 6 shows the electron density profiles calculated from the structure factor amplitudes for DPPC $L_{\beta'}$ gel bilayers (Figure 6A) and DHPC gel lamellae (Figure 6B) at 20 °C. The phase assignment used for the four structure factors obtained from scattering intensity data of DPPC bilayers, (−, −, +, −), is that reported previously (Ruocco et al., 1983). The phases for the structure factor amplitudes for DHPC lamellae, (−, −, +), were assigned by using Figure 1 of McIntosh et al. (1983). It should be noted that an identical structure factor phase sequence, (−, −, +, ±), for interdigitated β-DPPC lamellae has also been recently reported (Serrallach et al., 1983). Other possible phase combinations gave rise to electron density profiles which could be ruled out on physical grounds. The best-fit electron density profile corresponding to the phase sequence (−, −, +) is depicted in Figure 6B.

The differences between DPPC and DHPC gel-phase electron density profiles at 20 °C are remarkable. The DPPC bilayers exhibit an intrabilayer peak to peak separation, d_{pp}, of 43.5 Å and a central, low electron dense trough corresponding to the terminal methyl groups at the bilayer center. These structural characteristics have been reported earlier for PC bilayers (Levine et al., 1968; Inoko & Mitsui, 1978; McIntosh, 1978; Ruocco et al., 1983). In contrast, DHPC electron density profiles exhibit an intrabilayer peak to peak separation of 30 Å, as well as a central electron density distribution characteristic of interdigitated hydrocarbon chains (Ranck et al., 1977; Serrallach et al., 1983; McDaniel et al., 1983; McIntosh et al., 1983). A similar profile is obtained at −2 °C (not shown). The key feature of the one-dimensional electron density profile for DHPC is the central density distribution which is *not* observed if the hydrocarbon chains are tilted with respect to the bilayer normal in a noninterdigitated bilayer [compare Figure 6A (noninterdigitated) with Figure 6B (interdigitated)]. From the lipid layer thickness ($d_{pp} \sim d_l = 30$ Å), a molecular surface area (S) per DHPC molecule of 79 Å^2 is calculated. Calculation of the chain cross-sectional area, $\Sigma = 2s^2/\sqrt{3}$ where $s = 4.04$ Å, yields $\Sigma = 18.8$ Å^2, which translates into a ratio of area per DHPC molecule per hydrocarbon chain of $S/\Sigma = 4.2$.[2] Such ratios are observed for phospholipid interdigitated lamellar phases (Ranck et al., 1977; Serrallach et al., 1983; McDaniel et al., 1983). Similar structural parameters are obtained for interdigitated DHPC gel lamellae at −2 °C. At −2 °C, the persistence of axially symmetric ^{31}P NMR line shapes characteristic of diffusion rates $>10^5$ s^{-1} (Griffin, 1981) is clearly consistent with a greater molecular surface area compared to DPPC "crystal" (L_c) bilayers ($S \sim 38$ Å^2/DPPC (Ruocco & Shipley, 1982b), which allows the phosphocholine head group of DHPC to continue to diffuse rapidly at lower temperatures.

Comparing ^{31}P NMR spectra of DPPC and DHPC at representative temperatures in the gel (31 °C) and liquid-crystalline (50 °C) phases, Hauser (1981) concluded that the motionally averaged conformation of the phosphocholine head group was identical in both lipids, independent of the type of linkage to the glycerol backbone. A more complete study of the temperature dependence of the ^{31}P NMR line shapes in both lipids presented in this study corroborates the earlier observations of Hauser (1981) and Siminovitch et al. (1983) but reveals that at lower temperatures, in the lamellar phase of each lipid, and particularly in the phases below the low-temperature subtransitions, there are dramatic differences in the ^{31}P NMR line shapes.

The ^{31}P spectrum of DPPC in the subphase at −2 °C (Figure 5) is in agreement with previously published line shapes of DPPC in the subphase (Füldner, 1981; Lewis et al., 1984). In contrast to the *axially symmetric* powder line shapes which are observed in DHPC down to at least −20 °C, the DPPC line shapes indicate reorientation of the PO_4 moiety at an intermediate exchange rate ($\omega\tau_c \approx 1$) of 10^4–10^5 s^{-1} (Campbell et al., 1979). Using the diffusion model of Campbell et al. (1979), Füldner (1981) concluded that reorientation of the PO_4 moieties occurs at a significantly slower rate in the subphase as compared with the $L_{\beta'}$ phase. The DHPC spectra in Figures 4 and 5 demonstrate that ^{31}P NMR *cannot* detect the reversible, low-enthalpy transition at 4 °C identified by DSC and thus suggest that there is very little change in the rate of reorientation of the PO_4 moiety in the DHPC subphase.

[2] $S = 2(M\bar{v}/d_l N_A)10^{-24}$ where $\bar{v}$, the partial specific volume for DHPC ($\bar{v} \sim 0.98$ mL/g), was estimated by taking the reduced head-group volume for ether-linked PC ($V = 320$ Å^3) compared to that for DPPC ($V = 340$ Å^3) (Schwarz et al., 1976) into consideration, M is the molecular weight of DHPC (724), N_A is Avogadro's number, and d_l is the lipid layer thickness.

The observation of axially symmetric powder patterns, characteristic of rapid axial diffusion on the ^{31}P NMR time scale ($>10^5$ s^{-1}), down to $\sim$−30 °C in DHPC suggests that long-axis diffusion persists to much lower temperatures in DHPC than in DPPC. In DPPC-d_{62}, Davis (1979) has shown that axial diffusion continues to decrease and stops on a ^2H NMR time scale at about −7 °C. In this same temperature range, ^{31}P (Griffin et al., 1978) and ^{13}C (Wittebort et al., 1981) NMR spectra are no longer axially symmetric, again showing that the axial diffusion rate has decreased. It is certainly not coincidental that just below 0 °C in DPPC, there is a disappearance of the ^{14}N NMR signal from the choline head group as the spectra become severely broadened and the decay of the quadrupolar echo becomes very short (Siminovitch et al., 1983). Indeed, these changes have been attributed by Siminovitch et al. (1983) to a decrease in the rate of axial diffusion. The authors concluded that this same process occurs at a much lower temperature in DHPC, since the disappearance of the ^{14}N NMR signal occurs about 20 °C lower. It would now appear that a persistence of long-axis diffusion to much lower temperatures in DHPC than in DPPC can provide a unified explanation of the ^{14}N NMR results (Siminovitch et al., 1983) and the ^{31}P NMR results presented here.

The major differences observed in the X-ray diffraction patterns and ^{31}P NMR spectra of the low-temperature gel phases of DHPC are probably a manifestation of conformational differences at the glycerol backbone as a result of replacing the ester sp^2 carbon of the carbonyl group with an sp^3 carbon of the alkyl hydrocarbon chain. Solid-state ^2H NMR studies of DHPC specifically labeled in the choline head group and in the hydrocarbon chains are in progress to further elucidate specific conformational differences between DPPC and DHPC in bilayers. The effects of an equimolar concentration of cholesterol in DHPC bilayers, which are no longer interdigitated in the presence of 50 mol % cholesterol, are also under study.

ACKNOWLEDGMENTS

We thank Drs. G. G. Shipley and T. J. McIntosh for useful discussions. We acknowledge Dr. D. M. Small for making available the facilities of the Biophysics Institute at the Boston University School of Medicine. We also thank Dr. D. Atkinson for use of the X-ray diffraction facilities, D. Jackson for technical assistance, and Anne Lawthers for preparation of the manuscript.

Registry No. DPPC, 63-89-8; DHPC, 36314-47-3.

REFERENCES

Albert, D. H., & Anderson, C. E. (1977) *Lipids 12*, 188–192.
Bittman, R., Clejan, S., Jain, M. K., Deroo, P. W., & Rosenthal, A. F. (1981) *Biochemistry 20*, 2790–2795.
Boggs, J. M., Stamp, D., Hughes, D. W., & Deber, C. M. (1981) *Biochemistry 20*, 5728–5735.
Campbell, R. F., Meirovitch, E., & Freed, J. H. (1979) *J. Phys. Chem. 83*, 525–533.
Chen, S. C., Sturtevant, J. M., & Gaffney, B. J. (1980) *Proc. Natl. Acad. Sci. U.S.A. 77*, 5060–5063.
Cho, K. C., Choy, C. L., & Young, K. (1981) *Biochim. Biophys. Acta 663*, 14–21.
Davis, J. H. (1979) *Biophys. J. 27*, 339–358.
Füldner, H. H. (1981) *Biochemistry 20*, 5707–5710.
Griffin, R. G. (1981) *Methods Enzymol. 72*, 108–174.
Griffin, R. G., Powers, L., & Pershan, P. S. (1978) *Biochemistry 17*, 2718–2722.
Hauser, H. (1981) *Biochim. Biophys. Acta 646*, 203–210.
Hauser, H., Guyer, W., & Paltauf, F. (1981) *Chem. Phys. Lipids 29*, 103–120.
Hoerr, C. W., & Paulicka, F. R. (1968) *J. Am. Oil Chem. Soc. 45*, 793–797.
Howard, B. V., Morris, H. P., & Bailey, J. M. (1972) *Cancer Res. 32*, 1533–1538.
Howard, B. V., Butler, J. DeB., & Bailey, J. M. (1973) in *Tumor Lipids: Biochemistry and Metabolism* (Wood, R., Ed.) pp 200–214, American Oil Chemists Society Press, Champaign, IL.
Inoko, Y., & Mitsui, T. (1978) *J. Phys. Soc. Jpn. 44*, 1918–1924.
Janiak, M. J., Small, D. M., & Shipley, G. G. (1976) *Biochemistry 15*, 4575–4580.
Lakowicz, J. R., & Hogen, D. (1981) *Biochemistry 20*, 1366–1373.
Lee, T., & Fitzgerald, V. (1980) *Biochim. Biophys. Acta 598*, 189–192.
Levine, Y. K., Bailey, A. I., & Wilkins, M. H. F. (1968) *Nature (London) 220*, 577–578.
Lewis, B. A., Das Gupta, S. K., & Griffin, R. G. (1984) *Biochemistry 23*, 1988–1993.
Lutton, E. S. (1950) *J. Am. Oil Chem. Soc. 27*, 276–281.
Magni, R., & Sheridan, J. P. (1982) *Biophys. J. 37*, 11a.
McDaniel, R. V., McIntosh, T. J., & Simon, S. A. (1983) *Biochim. Biophys. Acta 731*, 97–108.
McIntosh, T. J. (1978) *Biochim. Biophys. Acta 513*, 43–58.
McIntosh, T. J., McDaniel, R. V., & Simon, S. A. (1983) *Biochim. Biophys. Acta 731*, 109–114
Norton, W. T. (1981) *Adv. Neurol. 31*, 93–121.
Paltauf, F., Hauser, H., & Phillips, M. C. (1971) *Biochim. Biophys. Acta 249*, 539–547.
Rance, M. A., & Byrd, R. A. (1983) *J. Magn. Reson. 52*, 221–240.
Ranck, J. L., Keira, T., & Luzzati, V. (1977) *Biochim. Biophys. Acta 488*, 432–441.
Rouser, G., & Yamamoto, A. (1968) *Lipids 3*, 284–287.
Ruocco, M. J., & Shipley, G. G. (1982a) *Biochim. Biophys. Acta 684*, 59–66.
Ruocco, M. J., & Shipley, G. G. (1982b) *Biochim. Biophys. Acta 691*, 309–320.
Ruocco, M. J., Shipley, G. G., & Oldfield, E. (1983) *Biophys. J. 43*, 91–101.
Schwarz, F. T., & Paltauf, F. (1977) *Biochemistry 16*, 4335–4339.
Schwarz, F. T., Paltauf, F., & Laggner, P. (1976) *Chem. Phys. Lipids 17*, 423–434.
Serrallach, E. N., Dijkman, R., de Haas, G. H., & Shipley, G. G. (1983) *J. Mol. Biol. 170*, 155–174.
Siminovitch, D. J., Jeffrey, K. R., & Eibl, H. (1983) *Biochim. Biophys. Acta 727*, 122–134.
Siminovitch, D. J., Ruocco, M. J., & Griffin, R. G. (1984) *Biophys. J. 45*, 197a.
Sunder, S., Bernstein, H. H., & Paltauf, F. (1978) *Chem. Phys. Lipids 22*, 279–283.
Tardieu, A., Luzzati, V., & Reman, F. C. (1973) *J. Mol. Biol. 75*, 711–733.
Vaughan, D. J., & Keough, K. M. (1974) *FEBS Lett. 47*, 158–161.
Wittebort, R. J., Schmidt, C. F., & Griffin, R. G. (1981) *Biochemistry 20*, 4223–4228.